OPTIMIZATION OF FLUE GAS DESULPHURIZATION ABSORBER BY MEANS OF CFD ANALYSIS

Katolicky J. and Jicha M.*
*Author for correspondence
Faculty of Mechanical Engineering,
Brno University of Technology
Brno, 61669,
Czech Republic,
E-mail: jicha@fme.vutbr.cz

ABSTRACT

In the paper we present an optimization study/retrofit of the flue gas desulphurization (FGD) absorber focusing on the flow field in the desulphurization vessel and the performance of the rotary atomizer used there. The study is performed using CFD code with a well validated model for the semi-dry desulphurization. For the numerical modeling of the multiphase flow in the absorber, the Euler-Lagrange approach is used with the Eddy Interaction Model. The numerical study focuses on the optimization of the flow field inside the absorber with the aim to increase the time during which the lime slurry remains in contact with flue gases.

Results of the numerical modelling are in very good agreement with operational tests.

INTRODUCTION

The semi-dry desulphurization process used in the retrofitted plant combines pros and cons of wet and dry processes, and is ranked the second behind wet scrubbers. Compared to the wet scrubbers, the semi-dry one has lower capital costs and higher operational costs mainly due to the use of a more expensive sorbent lime. The semi-dry process can be combined with a dry sorbent injection directly in the flue gas prior to the absorber reactor vessel in order to increase the efficiency of SO_2 removal.

The volume of the absorber is the main place where the desulphurization process runs. A water suspension (lime slurry) is sprayed into the absorber. The desulphurization process takes place on the wet droplet that contains thousands of micro particles of sorbent and this process results in a dry powder product. The suspension is prepared from lime hydrate, water and eventually from a recycled dry desulphurization product. The ratio of lime hydrate in the desulphurization suspension is controlled by the SO_2 concentration in the flue gases and the outlet gas temperature is controlled by the sprayed water mass.

The water suspension is sprayed into the absorber either by pressure injectors arranged as a multi-injector spraying system to cover as large a cross section of the absorber as possible or by rotating atomizers. In the current retrofit, we selected one centrally placed rotating atomizer with a rotating wheel equipped with a number of radial channels through which the water slurry is sprayed into the absorber vessel at its top. The size spectrum of water slurry droplets is controlled mainly by the rotational speed of the wheel.

As the absorber subjected to the retrofit deals with the semi-dry process, we eliminated the wet process from our study and focused on technologies that can be applied easily and without high installation costs. These are mainly technologies that use circulating fluidized bed reactors [1, 2], or a magnetically fluidized bed reactor [3] or a spouted bed reactor [4, 5]. We also considered appropriate the technology that utilises coal ash directly as the desulphurization sorbent activated by spray water [6]. The main idea of these technologies lies in bringing the flue gas into as perfect a contact with the sorbent as possible, and in increasing the residence time of flue gases in the zone of the high sorbent concentration.

Several modeling approaches to FGD can be found in the literature. In the article by Scala et al. [7], the authors use a one-dimensional spray-dryer model to predict the influence of several operating variables on the desulphurization performance. In the article by Wang [6], a humidified coal ash is used as the desulphurization sorbent and desulphurization efficiency is predicted by the 3D Euler/Lagrange modeling approach. Marocco and Inzoli [8] employed an Euler-Lagrange approach to model a two phase flow in wet FGD along with a model for droplet/wall interaction. Several studies show that the droplets size is a significant parameter, but we can hardly find relevant data that explicitly show how the quality of the spray influences the sulfur capture efficiency.

NOMENCLATURE

App	[m^2]	Droplet cross-sectional area,
Ap	[m^2]	Droplet surface
A_{ag}	[m]	Area of the projected droplet
c	[J/kg K]	Thermal capacity
C_D	[-]	Drag coefficient
d_p	[m]	Droplet diameter
d	[m]	Rotary wheel diameter
d_{ag}	[m]	Dry agglomerate diameter
d_I	[m]	Diameter of the reaction front
d_t	[m]	Diameter the nozzle channel in the rotary wheel
D_{SO2}	[m^2/s]	Diffusion coefficient
h_l	[J/kg]	Latent heat of evaporation
k	[W/mK] [-]	Thermal conductivity and number of nozzles in the rotary wheel
m_p	[kg]	Mass of droplet
$m_{p,ev}$	[kg]	Evaporated mass
m	[kg/s]	Mass flow
p	[Pa]	pressure
$\mathbf{U}_\infty$	[m/s]	Free stream velocity
$\mathbf{Up}$	[m/s]	Droplet velocity
t	[s]	Time

T_p	[K]	Droplet temperature
w	[kg/m^3]	Mass concentration
x	[m]	Cartesian axis direction
y	[m]	Cartesian axis direction
z	[m]	Cartesian axis direction

Special characters

β_g	[m/s]	Mass transfer coefficient
ϕ	[N/A]	General variable in the conservation equations
Γ	[N/A]	General effective (sum of molecular and turbulent) diffusion coefficient
ρ_∞	[kg/m^3]	Free stream density
ω	[m/s]	Angular velocity

Subscripts

∞	Free stream
p	Droplet

NUMERICAL MODEL FOR TWO-PHASE FLOW AND DESULPHURIZATION

Flow field

A detailed description of the two-phase flow and desulphurization model is given in Katolicky and Jicha [8]. For the numerical solution of the flow field in the desulphurization absorber, a commercial CFD program StarCD was used to solve the two-phase flow with a user defined desulphurization model and spray boundary conditions. The two-phase flow was solved using the Eulerian-Lagrangian approach with stochastic particle tracking. A continuous phase of the particle-laden turbulent flow is traditionally approached using the Reynolds-averaged Navier-Stokes (RANS) equations for mass, momentum, and energy conservation:

$$\frac{\partial}{\partial x_i}\left(\rho u_i \varphi\right) = \frac{\partial}{\partial x_i}\left(\Gamma \frac{\partial \varphi}{\partial x_i}\right) + S_\varphi + S_\varphi^P \qquad (1)$$

The source term S_φ contains internal sources such as mass transferred between phases (evaporation) in the continuity equation or various forces acting on the fluid. S_φ^p is the source arising from the particulate phase that is solved using the Lagrangian approach. Turbulence was modelled with a standard k-ε two equation turbulence model.

A discrete phase was solved using Lagrange equations for mass, momentum, and energy. These equations are solved for a cloud of computational particles; their position, mass, velocity and temperature are evaluated along the particles trajectory when they fly through the set of control volumes of the continuous phase. Changes in the mass, momentum, and energy are then transported into the continuous phase in the form of additional sources S_φ^p. The conservation of momentum for discrete particles in continuous flows is often referred to as B-B-O equation (Basset, Boussinesq and Oseen) and can be expressed as the balance of forces acting on the particle in the following way:

$$m_p \frac{d\mathbf{U}_{p,i}}{d} = \frac{1}{2}{}_t\rho_\infty C_D A_p \left|\mathbf{U}_\infty \underset{p}{-} \mathbf{U}_{p,i}\right|\left(\mathbf{U}_\infty - \mathbf{U}_{p,i}\right) + m_p \mathbf{g} \; (2)$$

Similarly to the momentum source, the thermal energy is tracked along the particles trajectory and a source term into energy equation is calculated. In our case, only a convective heat transfer between the particles and the surrounding fluid was considered. The transfer of latent heat during evaporation must also be taken into account. The energy equation for a particle temperature change can be written:

$$\frac{dT_p}{dt} = \frac{Nu}{\tau_T}\left(T_\infty - T_p\right) - \frac{1}{\tau_T}\frac{h_l}{\pi d_p k_\infty}\frac{dm_{p,ev}}{dt} \qquad (3)$$

The Nusselt number Nu is calculated from the Ranz-Marshall [9] formula for solid sphere. τ_T is the relaxation time for temperature and reads

$$\tau_T = \frac{\rho_p c_p d_p^2}{6k_\infty} \qquad (4)$$

The evaporated mass flow of water for the individual particles is calculated from the following equation:

$$\dot{m}_{p,ev} = \pi d_p^2 \beta_g \, p \ln\left(\frac{p - p_\infty}{p - p_s}\right) \qquad (5)$$

Desulphurization model

A desulphurization model solves the simultaneous water phase evaporation from the surface of individual droplets and the transfer of sulfur dioxide from the flue gases at the droplet-gas interface.

The overall balance of sulphur dioxide transport from flue gases into the droplets formed by lime slurry is given by a chemical reaction between sulphur dioxide SO_2 and calcium hydroxide $Ca(OH)_2$

$$SO_2(g) + Ca(OH)_2 \rightarrow CaSO_3 \cdot ½\, H_2O + ½\, H_2O \qquad (6)$$

Concentrations of SO_2 in flue gases are solved as an active scalar from the following equation:

$$\frac{\partial\left(\rho u_i w_{SO2}\right)}{\partial x_i} = \frac{\partial}{\partial x_i}\left(\rho D_{SO2}\frac{\partial w_{SO2}}{\partial x_i} + \frac{\mu_t}{Sc}\frac{\partial w_{SO2}}{\partial x_i}\right) + S_{SO2} \qquad (7)$$

The last term on the right side S_{SO2} is a volumetric source term resulting from the transport of SO_2 between flue gases and the lime slurry droplet and is calculated from the mass flow rate of sulfur dioxide by the following equation:

$$\dot{m}_{SO_2} = \rho_\infty \beta_{g,SO2} A_p \left(w_{SO2,\infty} - w_{SO2,I}\right) \qquad (8)$$

The overall mass transfer coefficient $\beta_{g,SO2}$ of SO_2 between flue gases and the droplet is calculated from the formula according to Hill and Zank [10]:

$$\beta_{g,SO_2} = \left[\left(\beta_{o,SO2}\right)^{-1} + \left(\frac{D_{SO2}}{\varepsilon}\frac{S_{d_I}, d_{ag}}{A_{ag}}\right)^{-1}\right]^{-1} \qquad (9)$$

The efficiency of the desulphurization process is defined as a ratio of the mass flow rate of sulphur dioxide absorbed in lime slurry particles and the mass flow rate of sulphur dioxide entering the solution domain of the FGD reactor:

$$\eta = \frac{\dot{m}_{SO_2,in} - \dot{m}_{SO_2,out}}{\dot{m}_{SO_2,in}} \qquad (10)$$

GEOMETRY OF DESULPHURIZATION ABSORBER AND ROTARY ATOMIZER

Flow field

The absorber consists of two parts:

- Distribution part, located in the upper space of the absorber
- Absorber vessel where the desulphurization process takes place

The distribution part is composed of nine channels, which lead to three concentric conic chambers – see Fig. 1. In these chambers, vanes are located. The flow rate through the individual channels is controlled by dampers.

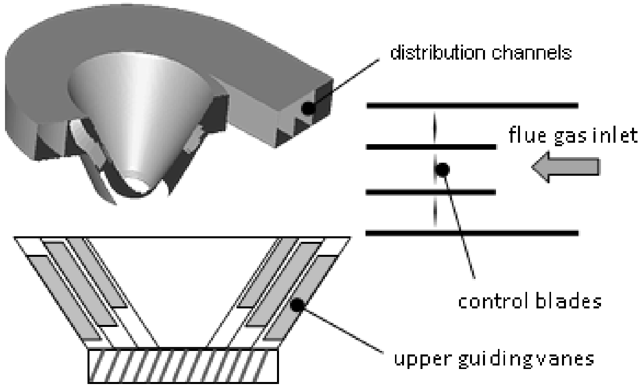

Fig.1. Scheme of multi-blade control dumper

In the upper part of the absorber vessel, a rotary atomizer is located; it distributes lime slurry into the absorber. The outlet of flue gases is located in the lower part of the absorber. The diameter of the cylindrical part of the absorber vessel is 12.6 m and the height 12.8 m. The absorber envelope is thermally insulated.

Rotary atomizer

The rotary atomizer (see Fig. 2) sprays the water slurry into the absorber. The advantage of the rotary atomizer lies in the ability to handle large flow rates and control relatively easily the size spectrum of lime slurry droplets by changing the rotary wheel revolutions. The rotary atomizer is placed in the upper part of the vessel where it distributes a mixture of calcium hydrate $Ca(OH)_2$ and water in flue gases. The lime slurry is sprayed through 16 radial channels (nozzles) into the absorber. For the numerical solution of the two-phase flow in the absorber, spray characteristics are needed i.e. the size spectrum, droplets velocity and their direction when the lime slurry leaves the nozzles. To specify these parameters for inlet conditions, i.e. for a given flow rate, physical parameters of the lime slurry, the atomizer diameter and the number of revolutions, is not always an easy task.

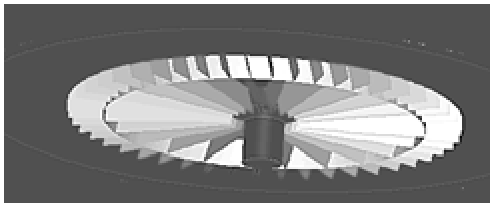

Fig.2. Rotary atomizer and lower distribution element with vanes

Several empirical formulas are available in the literature to calculate the mean droplet diameter (Sauter mean diameter SMD, D_{32}), radial velocity, and the influence of operational conditions for rotary atomizer. However, there are so large differences between the individual formulas that it is difficult to choose the one that would suit best. In the numerical solution described later, the Sauter mean diameter of 50 microns was chosen, which corresponds to the values by Kitamura [from 11]. When determining the size spectrum from the mean droplet diameter, we assume a log-normal distribution. Besides the size spectrum of the spray, the slurry velocity at the outlet from the nozzles is a paramount parameter as it principally influences the droplets trajectory and their residence time inside the absorber. The total velocity of the droplets that leave the nozzle in the rotary atomizer is a sum of radial and tangential velocity components. The tangential component is given by the rotational speed according to the formula

$$v_\tau = \pi \cdot d \, \frac{n}{60} \qquad (11)$$

A radial component is much more difficult to ascribe. The slurry that leaves the rotating wheel does not occupy the entire nozzle cross section but only a small part in the shape of a crescent. From this it follows that the outlet velocity will be much higher than that based on the total cross section. To specify the radial velocity, the following formula was taken [12]:

$$v_r = 0{,}758 \frac{\omega^{0,8} d^{0,4}}{B^{0,4}} \left(1 - \frac{0{,}943}{B^{0,95} \omega^{0,42} d^{1,43}} \right)^{0,4} \qquad (12)$$

B is a function defined as

$$B = 0{,}785 \cdot d_t^{0,35} \nu^{0,25} \left(\frac{k \cdot \rho}{\dot{m}} \right)^{0,8} \qquad (13)$$

NUMERICAL SIMULATIONS AND THEIR RESULTS – CURRENT OPERATIONAL REGIME

As mentioned above, the Sauter mean diameter of the whole spray was assumed d_{32}= 50 μm with the standard deviation s_g =

0.5. The size spectrum was divided into 5 size classes; for each of them a representing SMD was calculated in such a way that each of the sizes contained 1/5 of the total mass flow of the slurry. The slurry spray was imposed in total to 240 locations around the atomizer wheel and was formed in total by 1200 computational droplets; these were released into the absorber vessel with the appropriate radial and tangential velocity components. Simulations of the desulphurization process were run for several flow rates of flue gases; only one of them is presented in this article – see Table 1.

Table 1. Operational parameters

Flow rate of flue gases [kg/hour]	819,000
Temperature of flue gases [°C]	152
Water vapor content [%]	11.2
Concentration of SO2 [%] / [mg/Nm^3]	0.19 / 2320 0.38 / 4640

Flow mass of the lime slurry is controlled by the SO_2 concentration in the flue gases so that the ratio Ca/S is kept constant. The efficiency of the desulphurization changes according to the ratio Ca/S. In the graph in Fig. 3, the desulphurization efficiency can be seen as predicted by the numerical model for two different SO_2 concentrations and it is compared with the results from operational measurements.

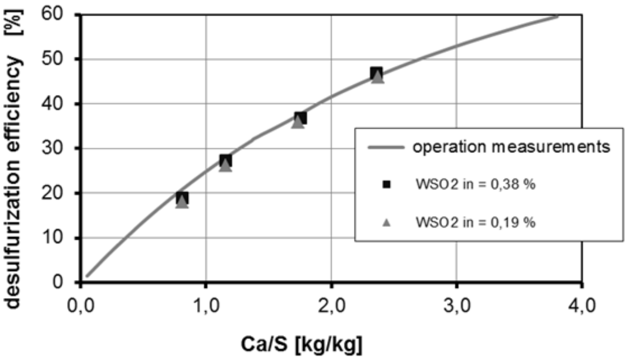

Fig.3. Desulphurization efficiency

NUMERICAL SIMULATIONS AND RETROFIT MEASURES

Based on a very detailed analysis of global 3D fields, a conclusion was made that it would be possible to improve the desulphurization efficiency simply by optimizing the global fluid flow of the flue gases in the absorber vessel by increasing the contact time of the lime slurry and flue gases, which may result in better desulphurization efficiency. Hence the main effort was paid to flue gases inlets. Several geometrical changes were made for inlet distribution diffuser and the vertical tilt of the vanes in the upper conical and lower cylindrical diffuser – see Fig. 4 and Table 2.

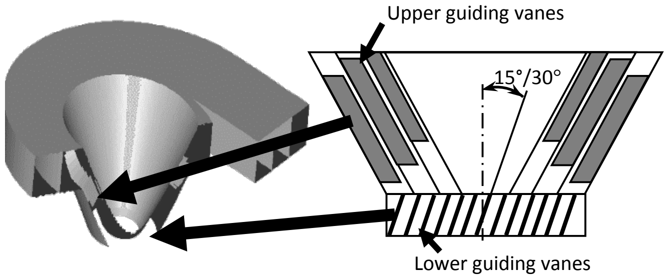

Fig. 4. Details of guiding vanes in the upper and lower distribution diffusers.

Table 2. Geometrical changes in guiding vanes

Set up of guiding vanes	Comments
DL15	Current set up of the vanes in the lower distribution element with 15° inclination
DL30	Inclination of the lower vanes set to 30° from the vertical
w/o1/3HL	Inclination of the lower vanes set to 15°, the outermost row of vanes removed in the upper conical diffuser
w/oHL	Inclination of the lower vanes set to 15°, all vanes removed in the upper conical diffuser
w/oH&DL	All vanes removed in both the upper and lower distribution diffusers

Results of desulphurization efficiency and SO_2 concentration are presented in Fig. 5 and 6, respectively As can be seen, the geometrical changes in the distribution diffuser led to the increase in efficiency, which ranges from about 3 % to 12%. The best efficiency was attained for the scenario in which both the upper and lower vanes were removed (w/oH&DL). The following in the ranking was the scenario of removed vanes in the upper conical diffuser (w/oHL).

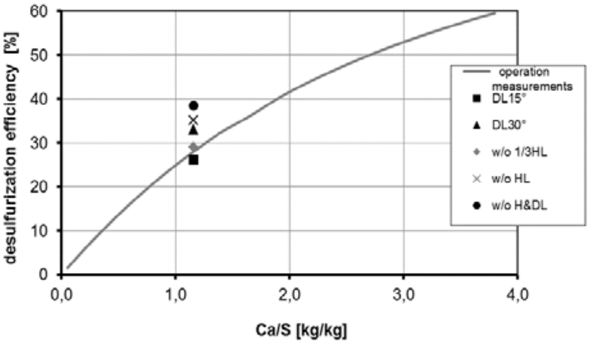

Fig.5. Desulphurization efficiency for different geometry of the vanes of distribution diffusers

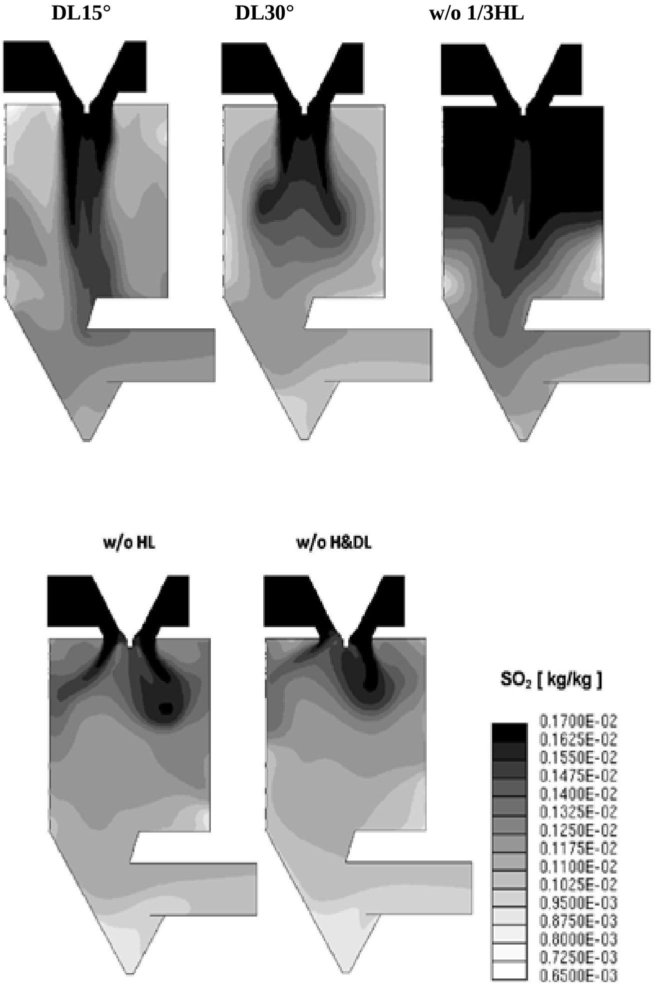

Fig.12. SO_2 concentrations in the absorber

CONCLUSION

In this article, the proposed model for semi-dry desulphurization enables us to calculate the desulphurization efficiency of the absorber equipped with a rotary atomizer. The main attention was paid to a global flow pattern in the absorber vessel in order to extend the residence time of flue gases in contact with the lime slurry. Several geometrical variants of the distribution diffuser that distributes flue gases into the absorber were studied with the aim to increase the contact time. The results show that a retrofit of semi-dry technology can be relatively simple and at low installation costs, with a reasonable desulphurization efficiency and calcium sorbent savings.

ACKNOWLEDGMENT

The authors gratefully acknowledge funding from the Ministry of Education, Youth and Sports of the Czech Republic under the National Sustainability Programme I (Project LO1202 NETME CENTRE PLUS) and the Brno University of Technology project of the specific research FSI-S-14-2355.

REFERENCES

[1] Hao X, Ma C, Dong Y, Yang J. Composite fluidization in a circulating fluidized bed for flue gas desulphurization, Powder Technol 2012;(215-216):46–53.

[2] Chen C, Li F, Qi H. Modeling of the flue gas desulphurization in a CFB riser using the Eulerian approach with heterogeneous drag coefficient, Chem Eng Sci 2012;69:659–668.

[3] Zhang Q, Gui K. A novel semidry flue gas desulphurization process with the magnetically fluidized bed reactor. J Hazard Mater 2009;168:1341–1345.

[4] Tao M, Jin B, Zhong W, Yang Y, Xiao R. Modeling and experimental study on multi-level humidifying of the underfeed circulating spouted bed for flue gas desulphurization. Powder Technol 2010;198:93–100.

[5] Rahimi A, Hatamipou MS, Gholami M, Haghnegahdar MR. Non-isothermal modeling of the flue gas desulphurization process using a semi-dry spouted bed reactor. Chem Eng Res Design 2011;89:777–784.

[6] Wang L, Song YB, Zhang MC, Fan HJ, Zhou YG, Fan WD, Wu J. Modeling study on the impaction and humidification process in desulphurization activation reactor. Chem Eng Sci 2005;60:951–962.

[7] Marocco L, Inzoli F. Multiphase Euler–Lagrange CFD simulation applied to Wet Flue Gas Desulphurisation technology, Int J Multiphase Flow 2009;35:185–194.

[8] Katolicky J, Jicha M. Influence of lime slurry droplets spectrum on the efficiency of semi-dry fluegas desulphurization using Euler-Lagrange approach, Chem Eng Technol 2013;36:156-166.

[9] Ranz WE, Marshall WR. Evaporation from drops, Part I, II. Chem Eng Proc 1952;48:141–146; 173–180.

[10] Hill FF, Zank J. Flue gas desulphurization by spray dry absorption, Chem Eng Proc 2000;39:45–52

[11] Mizuochi T, Akiyama T. ISIJ International 2003;43:1469-1471.

[12] Pazhi, D. G., Korjagin, A. A., Lamm, E. L. Atomization Device in Chemical Industry. Khimiya. Moscow. 1975 [in Russian].